Composite vortices of displaced Laguerre-Gauss beams

Daniel M. Kalb and Enrique J. Galvez

Department of Physics and Astronomy, Colgate University, 13 Oak Drive, Hamilton, New York 13346, U.S.A.

ABSTRACT

We report on the parametric study of composite-vortex patterns formed by displaced singly-ringed Laguerre-Gauss beams. We find that rich structures of vortices appear and disappear as the phase, topological charge and displacement of the component beams is varied. The net topological charge depends on various factors. When the beams are collinear or nearly collinear the net charge is the largest topological charge of the two component beams. When they are displaced by about one or more beam widths the net charge is the sum of the topological charges of the component beams plus the charge of vortices created by the shear phases in the region in between the two beams. The shear charges depend on the parameters of the problem. The experimental measurements are consistent with the expectations, although the measured location of the vortices is not necessarily in agreement with the predictions.

Keywords: Singular Optics, Optical Vortices, Laguerre Gauss beams

1. INTRODUCTION

Optical singularities are rich features of optical fields. They manifest in both scalar and vector forms.[1,2] Optical vortices are some of the most interesting types of scalar singularities. They have found new types of applications due to the orbital angular momentum that is carried by the optical field around them. In manipulation of matter they have been used to transfer angular momentum to matter.[1] They have also found use in the encoding of information in both the classical[3] and the quantal fields.[4]

Optical vortices are interesting because they allow the study of complex light beams from a different perspective. The study of their propagation has led to the discovery of interesting and unexpected dynamics, such as loops and knots in the trajectory of the singularities as the light propagates.[5–7] The beams that give rise to these features are produced by superpositions of Laguerre-Gauss (LG) beams, solutions of the wave equation in cylindrical coordinates.[8]

Our work has concentrated on the systematic study of the superpositions of two LG beams. Previously we studied the superposition of collinear beams carrying optical vortices.[9–11] In those studies, summarized in the second section, we found rich dynamics in the formation of new optical vortices. More recently we studied their propagation as the light went through a focal point.[11] We found that as the light was focused, off axis vortices rotated about the beam center due to the changing Gouy phases of the component beams.

In this article we report the study of composite-vortex beams that are generated when we add a new degree of freedom: a lateral displacement between the component LG beams. A previous analytical and numerical study of this problem for component beams with charges 0 and 1 showed that rich structures of vortices exist in the composite beams.[12] An important component of that work was to understand the values of the net topological charge of the composite beam. In our work we extend those studies to higher topological charges of the component beams. Our methods involve numerical modelings and experiments. Our findings broaden the understanding of the problem: the composite beams and the vortices contained within depend on whether the topological charges of the component beams have the same or opposite sign. Given this last important distinction we devote separate subsections to each case. We find that in both cases the structure of vortices and the net topological charge depends on the displacement and relative phase of the component beams.

Further author information: (Send correspondence to E.J.G.)
E.J.G.: E-mail: egalvez@mail.colgate.edu, Telephone: 1 315 228 7205
Proceedings of SPIE **7227**, (2009).

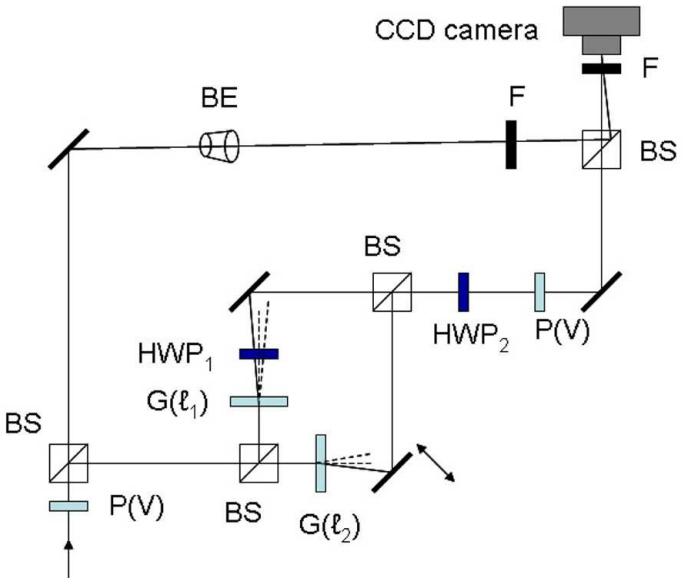

Figure 1. Schematic of the apparatus used to produce abd image the composite beams. The optical components include non-polarizing beam splitters (BS), forked diffraction gratings ($G(\ell)$) of topological charge ℓ, half-wave plates (HWP), polarizers (P), neutral density filters (F) and beam expander (BE).

2. OPTICAL ARRANGEMENT

In this work we do measurements of the composite beams to determine the location of the vortices contained in them. Since this setup is similar to previous ones,[9] we will describe it only briefly. The apparatus consisted of two nested Mach-Zehnder interferometers. Following Fig. 1, a vertically polarized helium-neon laser beam was split by a non-polarizing beam splitter in the outer interferometer. One of the beams was expanded and made interfere at an angle with the composite beam. This way it produced fringe interferograms, where the vortices were identified via the forks in the patterns.

The light in the other arm went through an inner Mach-Zehnder interferometer for preparing the composite beam. The light in each arm of the inner interferometer was incident on forked amplitude gratings with charges ℓ_1 and ℓ_2. First-order beams were then rerouted by the interferometer mirrors so that they exited the interferometer parallel to each other. The polarization of the light going through one of the arms was rotated by $\pi/2$ via a half-wave plate HWP_1. After the interferometer the polarization of the light was rotated via a second half-wave plate HWP_2 and then projected to the vertical direction via a polarizer. We could vary the relative intensity of the two beams by properly adjusting the orientation of HWP_2. For all the experiments reported here HWP_2 was oriented by $\pi/8$ relative to the horizontal so that the component beams combined with equal intensities. One of the mirrors of the interferometer was mounted on a translation stage with a piezo-electric inserted as a spacer. The beams were displaced by manually translating the stage. We adjusted the relative phase of the component beams δ by applying a voltage to the piezo-electric. The composite beams and their interference with the expanded reference beam were imaged with a CCD camera.

3. RESULTS

We will start the discussion by summarizing the results that are known for zero displacement of the component beams. Two singly-ringed LG beams with topological charges ℓ_1 and ℓ_2 ($|\ell_1| < |\ell_2|$) combine collinearly to produce a composite beam that has a central vortex of charge ℓ_1 surrounded by $|\ell_2 - \ell_1|$ peripheral vortices of charge $\sigma_2 = \ell_2/|\ell_2|$.[9] Small perturbations (i.e., the addition of a third weak beam) split the central vortex into $|\ell_1|$ vortices of charge $\sigma_1 = \ell_1/|\ell_1|$. The radial location of the peripheral vortices depends on the relative intensity of the component beams: $r = (w/\sqrt{2})[(|\ell_2|!I_1)/(|\ell_1|!I_2)]^{[1/2(|\ell_2|-|\ell_1|)]}$, where I_1 and I_2 are the intensities of the component beams. The angular separation of the peripheral vortices is $2\pi/|\ell_2 - \ell_1|$. Their absolute angular

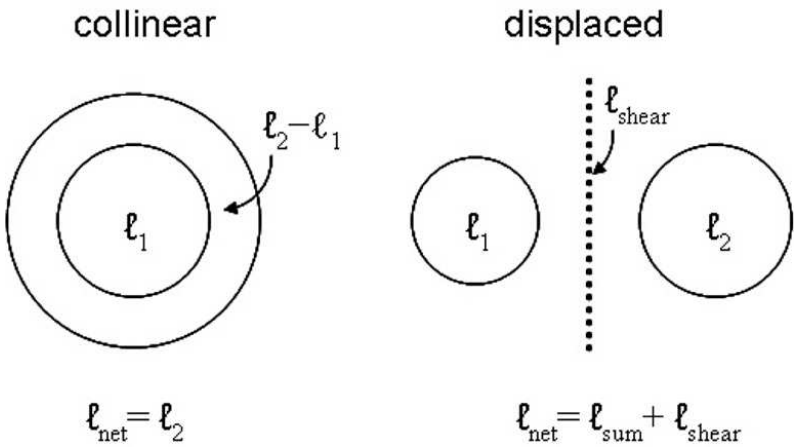

Figure 2. Schematic of the topological charges in the composite beam for the collinear and displaced cases (when $|\ell_1| \neq |\ell_2|$). In the collinear case it consists of a central region of charge ℓ_1 surrounded by a region of singly-charged vortices with a combined charge $\ell_2 - \ell_1$. In the displaced case there are three regions of vortices: around the center of each component beam, and in the region in between the two beams due to the shear in their phases.

location depends on the relative phase between the component beams[9]: $\phi = (\delta + n\pi)/(\ell_2 - \ell_1)$, where n is an odd integer. Since the topological charge of the central vortex is ℓ_1 and the combined charge of the peripheral vortices is $\ell_2 - \ell_1$ then the net topological charge of the beam is $\ell_{\rm net} = \ell_2$. This is shown schematically in Fig. 2.

When the beams are infinitely displaced their combined charge is $\ell_{\rm sum} = \ell_1 + \ell_2$. However, for finite separations the net topological charge is in general not $\ell_{\rm sum}$. This is because new phase dislocations appear if the phases of the two beams do not match up in the region between them. This phase mismatch is minimum when the component beams have topological charges of opposite sign. Conversely, when the topological charges of the component beams have the same sign, it is rather likely that there will be dislocations in the region between the beams. As depicted in Fig. 2, the region in between the two beams will in general contain shear charges with a net charge $\ell_{\rm shear}$. In the following subsections we consider the two cases in detail.

3.1. Case $\sigma_1 = -\sigma_2$

In this case the component beams have topological charges with opposite signs. We begin with a rather unique sub-case: when the component beams have equal and opposite charges (i.e., $\ell_1 = -\ell_2$). When the two beams are collinear and have equal intensities we get a mode that contains no vortices but $2|\ell_1|$ π-phase singularities angularly equidistant from each other. These shear singularities become vortices for infinitely small displacements of the two beams. As the displacement is increased from zero the vortices appear at the same angular locations as the shear singularities when the beams are collinear. They appear at a radial distance from the beam center equal to the radius of the beams ($r = w\sqrt{|\ell_1|/2}$, where w is the beam width).

We can understand this result with the following argument. As the displacement is increased the two beams stop sharing regions of equal phase. Thus, the regions of destructive interference cease to be radial lines and become points. The vortices occur where the amplitudes are the same and the phases off by π, which occurs near the ring maximum. Vortices of the same sign are adjacent to each other. The number of vortices is then $2|\ell_1|$, with half being of charge σ_1 and the other half of charge σ_2. Row (a) of Fig. 3 shows three frames describing the case when the component beams have topological charges $\ell_1 = 2$, $\ell_2 = -2$; a relative phase $\delta = 0$ and a displacement $\epsilon = 0.1w$. In this figure the left frames show a calculation of the gray-scale-coded phase map of the composite beam. The middle frames show the calculated intensity profile. The measured interferograms of the two beams are shown in the right frames. We have labeled the vortices that we identified in the interferograms with the symbols "$\circ$" and "$\times$" to denote topological charges $+1$ and -1, respectively.

The simulations of row (a) in Fig. 3 were done for the nearly collinear condition, where the displacement was $\epsilon = 0.1w$. The expectation was then to see two $+1$ charges on the left side of the image and two -1 charges

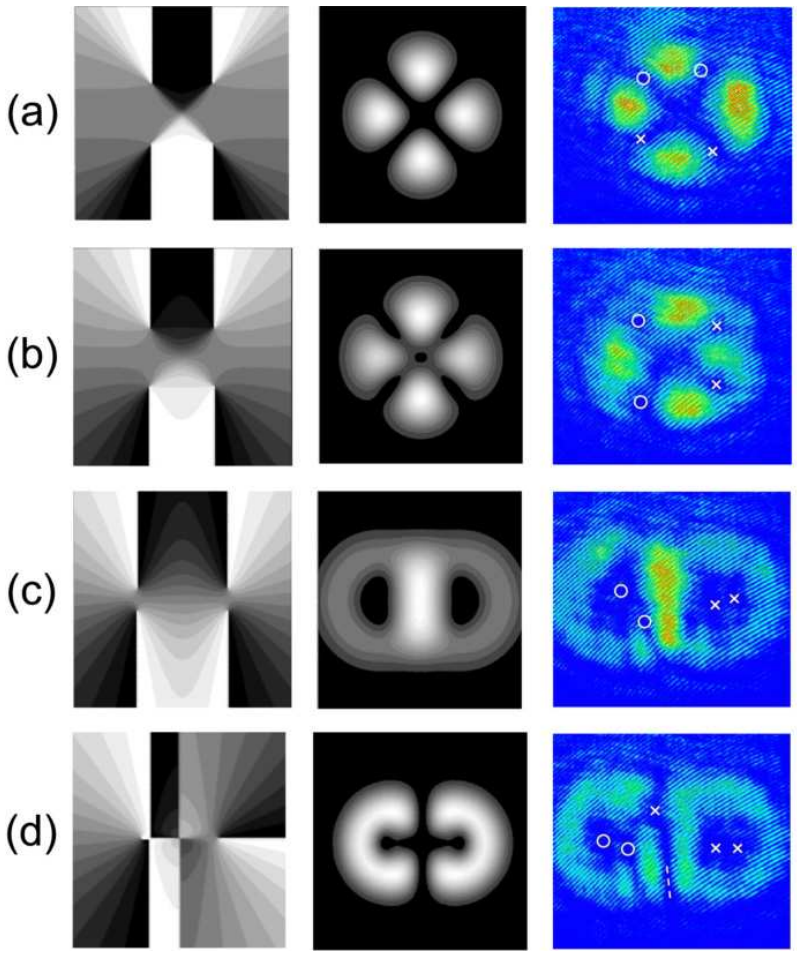

Figure 3. Numerical simulations of the phase (left column) and intensity (middle column) of the composite beams for cases where the component beams were $\ell_1 = -\ell_2 = 2$. Interferograms of the corresponding patterns are in the right column, with the location of vortices of charge $+1$ and -1 labeled by $\circ$ and $\times$, respectively. Rows (a)-(c) correspond to cases where $\delta = 0$ and the displacement is $\epsilon = 0.1w$ (a), $\epsilon = 0.3w$ (b), and $\epsilon = w$ (c). Row (d) corresponds to $\delta = \pi$ and $\epsilon = w$.

on the right side. This is not what was observed. However, we can explain this. Since this was very near the collinear condition a small unwanted vertical displacement changed the position of the vortices to the positions shown. Once the horizontal displacement increased to larger values (lower frames), then the vortices did appear at the expected locations.

If $\delta = 0$ for ℓ_1 even or $\delta = \pi$ for ℓ_1 odd, then the net charge of the composite beam remains $\ell_{\rm sum} = 0$ as the displacement is increased beyond the sum of the beam widths. One side of the composite will have $|\ell_1|$ vortices and the other side will have the same number of vortices with opposite sign. This is shown in rows (b) and (c) of Fig. 3, which correspond to the case $\delta = 0$ and an increasing displacement. The pattern and phases are confirmed by the interferograms of Fig. 3. In the region between the component beams the phase increases smoothly. This harmonious coexistence of the two component beams can be thought of as the analog of a pair of mechanical gears with their teeth matching up as they turn. This is illustrated in row (a) of Fig. 4, where we show a series of simulations of the phase map with increasing overall phase α of the two beams. Although the absolute phase is in general an irrelevant parameter, in the simulations it defines the location of the gray levels, allowing us to appreciate the phase structures generated by the two beams. The measurements for the cases of rows (b) and (c) in Fig. 3 are in general consistent with the simulations. The locations of the vortices are in the general area where they are expected. Slight discrepancies are due to imperfections of the wavefront

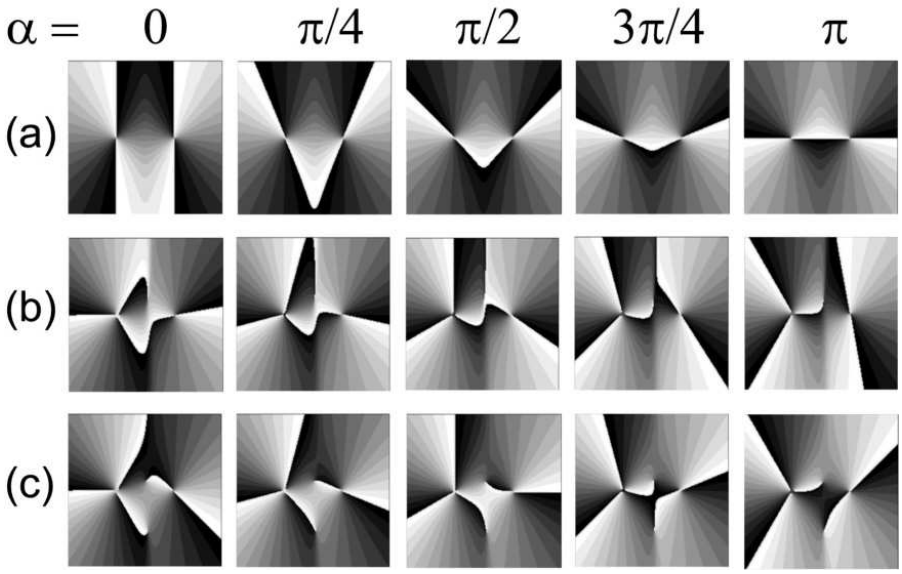

Figure 4. Numerical simulations of the phase of the composite beams for $\epsilon = 1.5w$, as a function of the overall phase α of the two component beams. The cases shown are: (a) $\ell_1 = +2$, $\ell_2 = -2$, $\delta = 0$; (b) $\ell_1 = -2$, $\ell_2 = +3$, $\delta = 160°$; (c) $\ell_1 = +2$, $\ell_2 = +3$, $\delta = \pi/2$.

of the beams. The reference beam used to produce the fringe patterns also acts as a perturbation that changes the positions of the vortices.

If the phase difference between the two beams for this case is changed to be near $\delta = \pi$ the situation changes. There will be a stressful region of phase in between the beams giving rise to either shear regions or pairs of oppositely-charged vortices. The net charge of the composite will still be $\ell_{\rm sum} = 0$. This is shown in the simulation of row (d) in Fig. 3. The interferogram shows an extra vortex in the upper middle part of the composite. In the lower part we were not able to identify a clear vortex, but noticed a region with a π-phase shear, denoted by the dashed line. A vortex could still be below it, but the beam was too weak to locate it.

When $|\ell_1| \neq |\ell_2|$ the beam in the collinear situation contains $|\ell_2 - \ell_1| + 1$ vortices. As the displacement is increased the central vortex of charge ℓ_1 splits into $|\ell_1|$ singly charged vortices, and then the beam has $|\ell_2 - \ell_1| + |\ell_1|$ vortices: $|\ell_2 - \ell_1|$ of charge σ_2 and $|\ell_1|$ of charge σ_1. If $|\ell_1|$ and $|\ell_2|$ differ by one or two, and if δ has a proper value, then when the beams are fully displaced there are $|\ell_1| + |\ell_2|$ singly charged vortices in the composite beam (i.e., with no shear vortices). What is interesting here is the transition: when going from collinear to non-collinear $|\ell_1|$ vortices of charge σ_2 *disappear*. An example of this for the case $\ell_1 = -2$, $\ell_2 = +3$ and $\delta = 0$ is seen in the transition from row (a) of Fig. 5, for $\epsilon = 0.1w$, to row (b) of Fig. 5, for $\epsilon = w$. How this transition occurs is rather interesting. Often a pair of vortices is created as the displacement is increased, with vortices with charge σ_1 annihilating the peripheral vortices of charge σ_2, and with the created partner moving out to radial distances that increase as the displacement is increased. Depending on the parameters the peripheral vortices may just move out of the beam as the displacement is increased. For the case of row (b) of Fig. 5 two of the peripheral vortices just moved away. The measurements show the disappearance of two +1 vortices (i.e., circles) in the transition from $\epsilon = 0.1$ (row (a)) to $\epsilon = w$ (row (b)).

For most other values of δ shear singularities or vortices appear in the region in between the component beams. Row (c) of Fig. 5 shows one such case, for $\ell_1 = -2$, $\ell_2 = +3$, $\delta = \pi$ and $\epsilon = w$. The measurements are somewhat consistent with this, as they show one oppositely charged vortex in between the two beams in addition to the three +1 and two −1 charges. The simulations predict the same number of vortices, but the experimental measurements do not find them exactly in the predicted locations.

It is difficult to specify a general rule since the outcome depends on the specific values of the parameters ℓ_1, ℓ_2, δ and ϵ. However, we can single out one rule that appears to remain: the sign of the shear vortices is the same

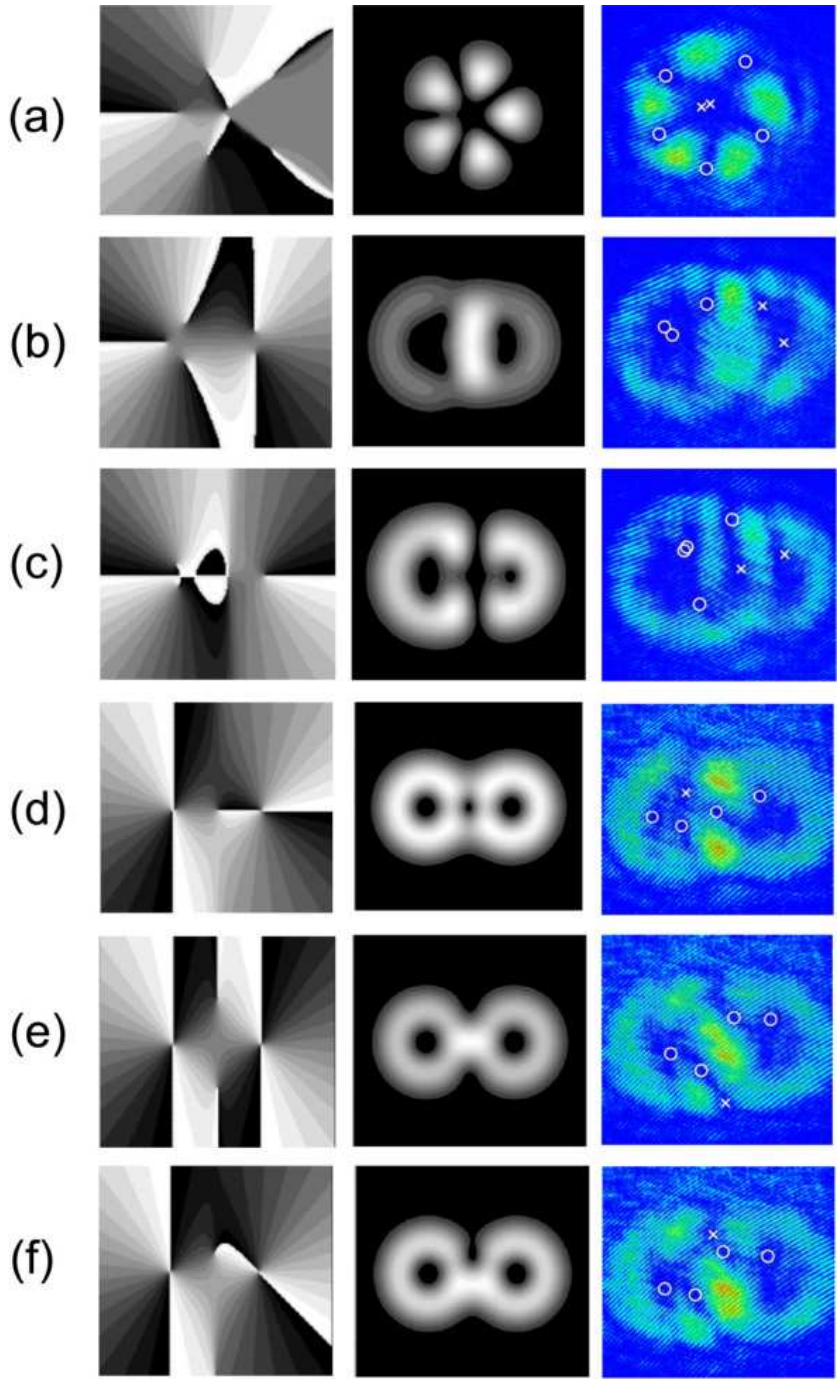

Figure 5. Numerical modeling of the phase (left column) and intensity (middle column); and measurements (right column) of composite vortices. The cases shown are: (a) $\ell_1 = -2$, $\ell_2 = +3$, $\delta = 0$ and $\epsilon = 0.1w$; (b) $\ell_1 = -2$, $\ell_2 = +3$, $\delta = 0$ and $\epsilon = w$; (c) $\ell_1 = -2$, $\ell_2 = +3$, $\delta = \pi$ and $\epsilon = w$; (d) $\ell_1 = \ell_2 = +2$, $\delta = \pi$ and $\epsilon = w$; (e) $\ell_1 = \ell_2 = +2$, $\delta = \pi$ and $\epsilon = w$; (f) $\ell_1 = \ell_2 = +2$, $\delta = \pi/2$ and $\epsilon = w$;

as ℓ_1. This is because the phase of a beam with charge ℓ_2 varies faster than the phase of the beam with charge ℓ_1. This is illustrated in the phase maps of row (b) in Fig. 4, where it can be seen that the phase mismatch between components with $\ell_1 = -2$ and $\ell_2 = +3$ causes a phase vortex of charge -1 in the region between the beams.

For the latter case, where there is one shear singularity of charge $\ell_{\rm shear} = -1$, the transition from collinear to displaced involves the disappearance of $|\ell_1| = 2$ charges with $\sigma_2 = +1$ and the appearance of a charge with $\sigma_1 = -1$. This is a net change of the net topological charge by $|\ell_1| + |\ell_{\rm shear}| = 3$.

3.2. Case $\sigma_1 = \sigma_2$

In this case the component beams have topological charges of the same sign. This case is quite complex because shear vortices are easily created in the region between the beams. If we ignore the shear vortices for a moment, as ϵ is increased from zero the composite pattern evolves from ℓ_1 central vortices and $|\ell_2 - \ell_1|$ peripheral vortices to $|\ell_1| + |\ell_2|$ vortices when the beams are displaced. Thus, at least $|\ell_1|$ vortices must *appear* in the transition. However, that transition also generates shear vortices of charge $-\sigma_1$. The number of shear vortices depends on the specific values of the parameters.

The simulations of row (c) in Fig. 4 show the phase maps for $\ell_1 = +2$ and $\ell_2 = +3$. One can clearly see two shear vortices with their sign opposite to that of the component beams. The change of the phase makes it clear how the shear vortices have the opposite sign. In that simulation we picked a value of delta close to π, at 160°. We did this because for $\delta = \pi$ there is a shear singularity and no vortices.

The case of $\ell_1 = \ell_2 = +2$ is an interesting one because the number of shear vortices depends on the relative phase of the component beams (i.e., δ). Rows (d), (e) and (f) of Fig. 5 show the cases where $\delta = 0$, $\delta = \pi$ and $\delta = \pi/2$, respectively. We see that when $\delta = 0, \pi$ there is only one phase singularity in the numerical simulations, while for $\delta = \pi/2$ there are two. In the first two cases the measured number of vortices is in agreement with the predictions, but their location is quite different. We cannot say with confidence whether this is due to the perturbing action of the reference beam or any other experimental systematic effects, such as misalignments or imperfections in the wavefront of the component beams. For the case where the simulations predict two vortices we see only one–the lower one. That the upper one does not show up should be no surprise because the beam intensity is low in the region where it is expected and is consequently difficult to image. Besides this discrepancy the experimental measurements do confirm the general features of the numerical modelings.

4. SUMMARY AND DISCUSSION

In summary, we have presented a new study of the composite-vortex patterns that arise when singly-ringed LG beams bearing optical vortices are combined together. The present study extends a previous study of collinear component beams to the case when the beams are parallel but displaced. We observe a number of interesting features in this parametric study: that for a given set of topological charges of the component beams vortices appear and disappear as the displacement is varied. The number and location of these vortices depends on the topological charges of the component beams and the relative phase between them. Presumably they also depend on the relative intensity of the two beams, but we did not performed that study.

There is a situation that may be of interest to investigate: when displaced vortices are focused by a lens. In this situation two component beams that are displaced will be steered to the focal spot where they will be a concentric and nearly collinear. After the focal spot the beams will diverge and become displaced again. In addition, the phase difference between the two beams will change due to the different Gouy phases of the component beams. We then envision a very rich situation where as the light propagates vortices are created and annihilated, and as they do this they rotate about the beam axis. It remains an open question whether knots could be produced this way. It appears that longitudinal loops formed by the creation and annihilation of vortex pairs of opposite sign will be present. The prospect of such interesting propagation dynamics makes this situation worthy of future study.

ACKNOWLEDGMENTS

This work was supported by a grant from Research Corporation.

REFERENCES

1. Andrews, D.L., *Structured Light and Its Applications: An Introduction to Phase-Structured Beams and Nanoscale Optical Forces*, (Academic Press-Elsevier, Burlington, 2008).
2. Soskin, M.S., and Vasnetsov, M.V., "Singular Optics," in *Progress in Optics 42*, E. Wolf, ed. (Elsevier 2001), pp. 219–276.
3. Gibson, G., Courtial, J., Padgett, M.J., Vasnetsov, M., Pas'ko, V., Barnett, S.M., and Franke-Arnold, S., "Free-space information transfer using light beams carrying orbital angular momentum," Opt. Express **12**, 5448–5456 (2004).
4. Molina-Terriza, G., Torres, J.P., and Torner, L., "Twisted Photons," *Nature Phys.* **3**, 305–310 (2007).
5. Berry, M.V., and Dennis, M.R., "Knotted and linked phase singularities in monochromatic waves," Proc. R. Soc. Lond. A **457** 2251–2263 (2001).
6. Berry, M.V., and Dennis, M.R., "Knotting and unknotting of phase singularitites: Helmholtz waves, paraxialwaves and waves in 2+1 spacetime," J. Phys. A **34** 8877–8888 (2001).
7. Leach, J., Dennis, M.R., Courtial, J., and Padgett, M.J., "Vortex knots in light," New J. of Phys. **7**, 1–11 (2005).
8. Allen, L., Beijersbergen, M.W., Spreeuw, R.J.C., and Woerdman, J.P., "Orbital angular momentum of light and the transformation of Laguerre-Gauss modes," Phys. Rev. A **92**, 8185–8189 (1992).
9. Galvez, E.J., Smiley, N., Fernandes, N., "Composite optical vortices formed by collinear Laguerre-Gauss beams," Proc. SPIE **6131**, 19–26 (2006).
10. Galvez, E.J., and Baumann, S.M., "Composite vortex patterns formed by component light beams with non-integral topological charge," Proc. SPIE **6905**, 6905D-1–7 (2008).
11. Baumann, S.M., MacMillan, L.H., Kalb, D.M., and Galvez, E.J., "Propagation Dynamics of Optical Vortices due to Gouy Phase," (to be published).
12. Maleev, I.D., and Swartzlander, Jr., G.A., "Composite optical vortices," J. Opt. Soc. Am. B **20**, 1169–1176 (2003).